Moiré contrast in the local tunneling barrier height images of monolayer graphite on Pt(111)

Masahiro Sasaki,* Yoichi Yamada, Yusuke Ogiwara, Shinjiro Yagyu, and Shigehiko Yamamoto
Institute of Applied Physics and Center for Tsukuba Advanced Research Alliance, University of Tsukuba, Tennoudai, Tsukuba, Ibaraki 305-8573, Japan
(Received 28 March 2000)

Moiré contrast between monolayer graphite and Pt(111) lattices is observed in local tunneling barrier height (LBH) images, where LBH's are calibrated with quasistatic I-z measurements. The observed Moiré amplitude of 1.6 eV, much larger than the possible maximum amplitude due to the electronic interference between lattices, suggests that there exists the spatial modulation of the microscopic work function of monolayer graphite in a nanometer scale originated from the interaction between layered adsorbate and substrate.

Monolayer graphite is a basic component of carbon-related materials, which are known to have unique properties for electron emission[1] and chemical reaction.[2] Much effort to study detailed geometrical and electronic behaviors of monolayer graphite has been made by means of several techniques. From a macroscopic point of view, Shelton, Patil, and Blakely and Zi-pu *et al.* have reported the geometrical structure of monolayer graphite studied by low-energy electron diffraction (LEED).[3,4] Aizawa *et al.* and Nagashima, Tejima, and Oshima have discussed the bond behavior of the monolayer graphite on the basis of the high-resolution electron-energy-loss spectroscopy (HREELS) observations.[5,6] From a microscopic point of view, Land *et al.* have demonstrated that there exists the Moiré contrast in the scanning tunnel microscope (STM) images of the monolayer graphite on Pt(111) surfaces.[7] However, there have been few reports on the microscopic electronic behaviors that are crucial to the electron emission and chemical reaction.

Local tunneling barrier height (LBH) imaging, which can be easily realized by STM equipment, has been pointed out by Binnig and Rohrer[8] to provide material-specific information in an atomic resolution, since the tunneling current decays with increasing the tip-sample separation at the decay constant of $2\kappa = 2\sqrt{2m\Phi_a}/\hbar$, where the value Φ_a, defined as LBH, is regarded as the average of the work functions of tip and sample surfaces in a simplified one-dimensional tunneling scheme. Thus, the microscopic electronic behaviors in an atomic scale have been discussed on the basis of the LBH observed for several adsorbate and substrate systems.[9–12]

In this paper, we report the microscopic electronic behaviors of the monolayer graphite on Pt(111) based on the LBH images that contain Moiré contrast similar to those for the STM images. The obtained LBH distributions, calibrated by quasistatic measurements, indicate that the surface microscopic work function is not homogeneous in a nanometer scale due to the interaction between monolayer graphite and substrate surface.

The experiments were carried out using an ultrahigh vacuum multichamber system that consists of an STM observation chamber, a surface treatment chamber, and a load-lock chamber.[11–12] The LBH image is obtained by calculating the value of

$$\Phi_a = 0.95[\mathrm{eV\AA}^2]\left(\frac{\Delta \log I}{\Delta s}\right)^2 \quad (1)$$

point by point, where the logarithmic deviation of tunneling current $\Delta \log I/\Delta s$ is measured by lock-in detection of the change in tunneling current of STM when the tip-sample separation is sinusoidally modulated at 6.25 kHz, well above the feedback frequency, under the constant current STM mode. Here, there is much ambiguity to determine the modulation amplitude Δs because of a relatively slow response of piezo devices and an unintentional mechanical vibrating resonance of the STM system. In this paper, we calibrate the LBH values from the quasistatic measurements where we simply measure the tunneling current as a function of the tip-sample separation when the tip is drawn up slowly at several lateral locations, and then derive the LBH values from the curve fittings of data.

The Pt(111) substrate (Mateck) is cleaned by a repeated procedure of Ar ion sputtering and annealing. The cleanliness is checked with LEED, Auger electron spectroscopy, and STM observations. Monolayer graphite is formed by exposing the clean Pt(111) surface with high purity ethylene of 50 L ($1\,\mathrm{L} = 10^{-6}\,\mathrm{Torr\cdot s}$) at room temperature and subsequently heating the sample up to 1200 K. The formation of monolayer graphite is confirmed with LEED observations.

Figure 1 shows the LBH image of the monolayer graphite on Pt(111) and its linescan along A-A' at the current of 1 nA and the tip bias of 10 mV. The brighter contrast in the LBH image, which means the higher LBH value, is observed at the topographically higher sites in the simultaneously observed STM image. We notice that the Moiré contrasts in the LBH images are much more distinct than those in the STM images.

In the LBH images as well as the STM images, we find two domains with atomic lattice directions different by 30° from each other. Only in the domain A, there exist Moiré contrasts with the period of 18 Å, which is similar to that has been reported by Land *et al.*[7] The Moiré period of 18 Å is checked with the spacing (2.13 Å) of the stripes corresponding to the graphite atomic arrangement. Since the difference in height between these domains is about 0.2 Å from the STM line profile, we consider that both the domains consist of monolayer graphite formed on the same Pt(111) terrace

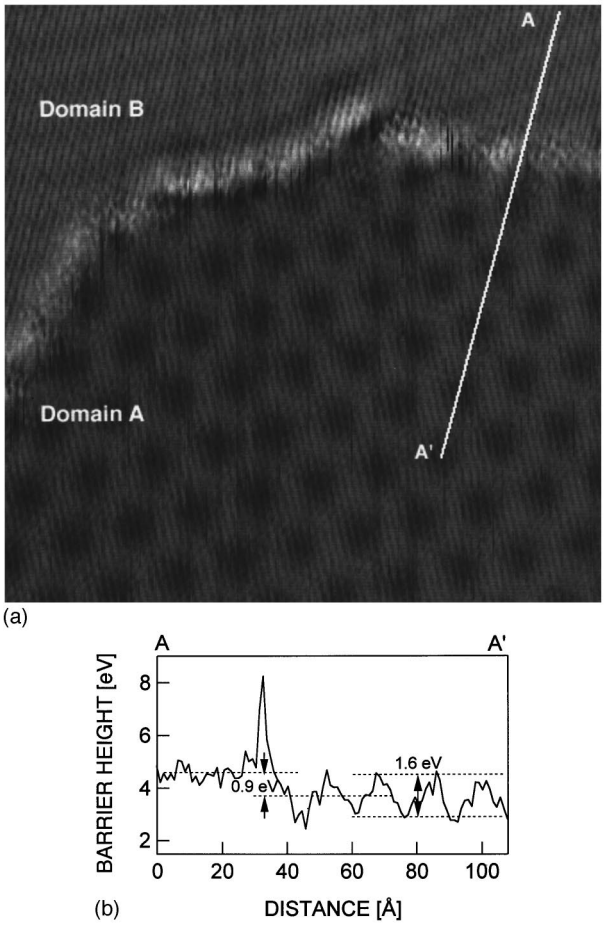

FIG. 1. 140 Å×140 Å LBH image (a) and its linescan (b) of the monolayer graphite on Pt(111) measured at the current of 1 nA and the tip bias of 10 mV. The LBH value is calibrated by the I-z data from the quasistatic measurements (Fig. 3). In the domain A, we observe the Moiré contrast whose period is 18 Å. In the domains A and B, we find the stripes for graphite atomic structure with the directions different by 30° from each other.

and the difference in geometrical height is possibly due to the change in the electronic properties.

The observed Moiré period of 18 Å is well reproduced by the superimposed Pt(111) and graphite lattices whose direction rotates by 4° as shown in Fig. 2(a). According to the difference of 30° in graphite direction between A and B domains, the graphite lattice in domain B rotates by 34° with respect to the substrate lattice. Under this geometry, the long-range Moiré contrast does not appear in the superimposed lattices [Fig. 2(b)], which is also consistent with the observed image without Moiré contrast.

The LBH values were calibrated from the quasistatic observations. Figure 3 shows the tunneling current as a function of tip-sample displacement that was measured when the tip was slowly drawn up at a position within the domain B. The tunneling current variations at the tip-surface separations adopted here are well reproduced by a single exponent in addition to a constant background. From the curve fittings of the tunneling current variations, we determine the LBH values. The values in the LBH image are calibrated on the basis of the I-z characteristics measured at tens of locations, providing the effective modulation amplitude of 1.0 $Å_{p\text{-}p}$. Consequently we confirm that the amplitude of the Moiré contrast is about 1.6 eV and the difference in mean LBH between domains A and B is about 0.9 eV. The obtained results may imply that the microscopic work function has a spatial periodic distribution in a nanometer scale. However,

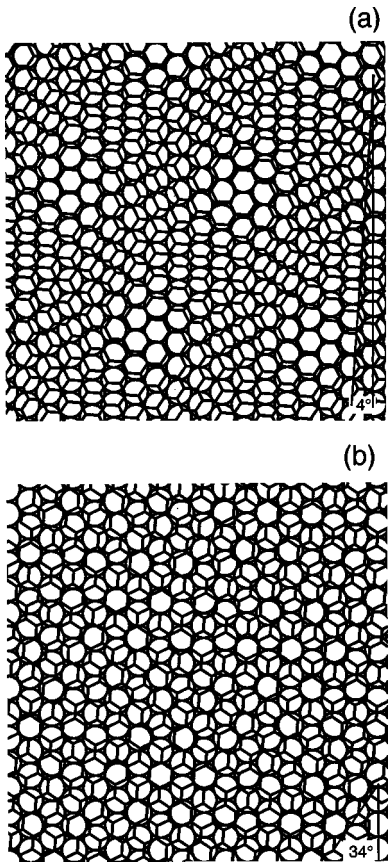

FIG. 2. Superimposed graphite and Pt(111) lattices, where the graphite atomic direction rotates with respect to the Pt(111) lattice by 4° (a) and 34° (b), which well reproduce the LBH contrasts for the domains A and B in Fig. 1(a) respectively.

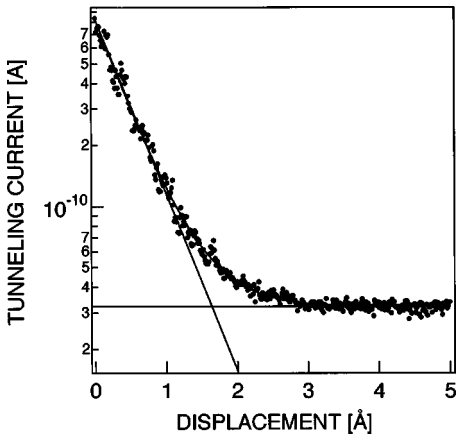

FIG. 3. Tunneling current as a function of the tip displacement at a position within the domain B (Fig. 1), which is obtained from the quasistatic measurement. The data is well fitted to a single exponent in addition to a constant background. From the tens of the measurements at different positions we calibrate the average LBH value.

since the apparent LBH distribution can appear without the change in microscopic work function from a view of the three-dimensional tunneling scheme, more detailed consideration is necessary.

Since the interlayer interaction of graphite is weak, it is expected that the monolayer graphite is not modulated by a substrate surface. Thus, we try to explain the observed Moiré contrast under the assumption that the work function of monolayer graphite remains homogeneous even after it is adsorbed on the Pt(111) surface. There can be an electron density modulation at the interface due to the interference in electronic structure between graphite and substrate periodicities, where we make no mention of the mechanism of the electronic modulation. According to the Tersoff's consideration,[13] the tunneling current is proportional to the electron density at the tip position at the Fermi level. In the three-dimensional tunneling scheme, the decay constant of the tunneling current with respect to the tip-sample separation is given by

$$2\kappa = 2\sqrt{2m(\Phi_{\mathrm{WF}} + E_{\parallel})}/\hbar, \tag{2}$$

where Φ_{WF} and $E_{\parallel}$ are the barrier height determined by the work functions (corresponding to the LBH value within the one-dimensional tunneling scheme) and the parallel component of kinetic energy (corresponding to the lateral periodicity), respectively. The parallel energy is given by

$$E_{\parallel} = \frac{\hbar^2}{2m}\left(\frac{2\pi}{a}\right)^2, \tag{3}$$

where a is the lateral period. Since the decay constant for the component of the Moiré periodicity is much smaller than that for the component of atomic periodicity, the electron density modulated by the interference can survive at the tip position, while the modulation due to atomic arrangement is decayed out, even when the amplitude of the electron-density modulation at the interface is small and the distance between interface and tip is so large.[13,14] The surviving modulation possibly results in the Moiré contrast in the STM image.

In general, also during the LBH observation, we sample the tunneling current consisting of the components with various parallel energies as well as the component with no parallel energy. Then the apparent LBH value (Φ_a) for each component is $\Phi_{\mathrm{WF}} + E_{\parallel}$, and the amplitude of each component is given by the local electron density for the component. To discuss the Moiré contrast, we need to take into account the components with the parallel energy for Moiré periodicity and with no parallel energy, which provide the apparent LBH's of $\Phi_{\mathrm{WF}} + E_{\parallel}$ and Φ_{WF}, respectively. Since the amplitude of the component for Moiré periodicity is laterally oscillated at the space frequency for the Moiré periodicity, it is possible that observed LBH value is modulated, resulting in the Moiré contrast, even under the framework of the homogeneous work function. It is noted that the observed LBH value must be in the range between $\Phi_{\mathrm{WF}} + E_{\parallel}$ and Φ_{WF}.

According to Eq. (3), the period of 18 Å of the Moiré contrast gives a parallel energy ($E_{\parallel}$) 0.47 eV, which is the possible maximum amplitude in apparent barrier height under the assumption of homogeneous work function. On the other hand, the amplitude of the Moiré contrast in the LBH image is observed to be 1.6 eV, much larger than the parallel energy for the Moiré period. Therefore, we conclude that the observed Moiré contrast cannot be explained under a homogeneous work function and consequently that the interaction between graphite and substrate is so strong that the microscopic work function of monolayer graphite is modulated in a nanometer scale. The modulation amplitude of 0.5–1.0 eV corresponding to the graphite *atomic* period in the LBH image (Fig. 1) may be explained by the difference in the amplitude of electronic components under the condition of homogeneous work function since the atomic periodicity provides such a high $E_{\parallel}$ as 24 eV.

From the careful comparison between the superimposed lattices [Fig. 2(a)] and the obtained LBH image [Fig. 1(a)], we find that the brighter areas in Fig. 2(a), where the carbon atoms in graphite sit at the hollow site of Pt(111) and consequently the center of the graphite hexagon is located on the top of the Pt atom, are arranged in the same period and symmetry as those for the dark area in the LBH images in Fig. 1(a). The carbon atoms at the Pt hollow sites are known to be highly stabilized from the several analytical methods.[15] This means that the microscopic work function becomes lower in case the carbon atoms in graphite are located near the hollow sites where carbon atom tends to make a strong interaction. Thus, it is considered from the LBH contrasts that the electrons in the graphite partially move towards the Pt substrates when the carbon atoms in graphite sit on the hollow sites. On the other hand, the higher LBH values in the domain *B* suggest that the interaction between the graphite and Pt atoms is not so strong in this domain, where the density of carbon atoms located near or at the Pt(111) hollow sites is very low. Therefore, the discussed features in the LBH images are simply understood by the interaction of graphite with Pt atoms dependent on the graphite location with respect to the substrate Pt atoms. Further, it should be noted that the contrasts in the STM images are consistently explained by the interaction of graphite and Pt(111). In Figs. 1(a) and 1(b), we also find that the LBH is extremely large at the domain boundary. This feature might be explained by electronic structure. More detailed systematic observations are required.

According to the HREELS observations by Aizawa *et al.*,[5] bond softening within the monolayer graphite, which occurs in the case of graphite on Ni(111), does not occur in the case of the graphite on Pt(111), indicating that the interaction of carbon with Pt substrate is weaker than that with Ni substrate. Aizawa *et al.* have explained the difference in softening by the geometrical arrangement, where an additional carbon layer is intercalated between substrate and graphite layer in the case of graphite on Pt(111). However, the indication of the carbon layer insertion has not been observed in the STM images. We speculate that the graphite on Pt(111) observed here is different in structure from those observed by HREELS.

Recently, Olesen *et al.* have reported that the constant apparent LBH as a function of tip-sample displacement is given by the interplay of the intrinsic lowering of LBH and the strong interatomic force between tip and sample at extremely small tip-sample separations.[16] In fact, the observed

I-z variation (Fig. 3) is well reproduced by a single exponent. However, in this paper we consider that the tip-sample separation is not so small according to a typical tunneling conductance of $10^{-7}\,\Omega^{-1}$. Therefore, the observed LBH variation is considered to be attributed to the real work function variation.

In conclusion, the microscopic work function of graphite on Pt(111) is not homogeneous and is well explained by the carbon locations with respect to the substrate Pt atoms. It should be also noted that the LBH imaging is effective to investigate the interaction between monolayer graphite and the substrate atoms.

*Electronic address: sasaki@bk.tsukuba.ac.jp

[1] For example: M. W. Geis, J. C. Twiehell, J. Macaulay, and K. Okano, Appl. Phys. Lett. **67**, 1328 (1995); A. G. Rinzler *et al.*, Science **269**, 1550 (1995); T. Asano, E. Shibata, D. Sasaguri, K. Makihara, and K. Higa, Jpn. J. Appl. Phys. **36**, L818 (1997).

[2] For example: S. M. Davis and G. A. Somorjai, *The Chemical Physics of Solid Surfaces and Heterogeneous Catalysis* (Elsevier, Amsterdam, 1982), Vol. 4, p. 294.

[3] J. C. Shelton, H. R. Patil, and J. M. Blakeley, Surf. Sci. **43**, 493 (1974).

[4] H. Zi-pu, D. F. Ogletree, M. A. Van Hove, and G. A. Somorjai, Surf. Sci. **180**, 433 (1987).

[5] T. Aizawa, Y. Hwang, W. Hayami, R. Souda, S. Otani, and Y. Ishizawa, Surf. Sci. **260**, 311 (1992).

[6] A. Nagashima, N. Tejima, and C. Oshima, Phys. Rev. B **50**, 17 487 (1994).

[7] T. A. Land, T. Michely, R. J. Behm, J. C. Hemminger, and G. Comsa, Surf. Sci. **264**, 261 (1992).

[8] G. Binnig and H. Rohrer, Surf. Sci. **126**, 236 (1983).

[9] R. Wiesendanger *et al.*, Surf. Sci. **189/190**, 24 (1987).

[10] Y. Hasegawa, J. F. Jia, K. Inoue, A. Sakai, and T. Skurai, Surf. Sci. **386**, 328 (1997).

[11] M. Sasaki, M. Komai, R. Ozawa, and S. Yamamoto, Jpn. J. Appl. Phys. **37**, 6186 (1998).

[12] M. Komai, M. Sasaki, R. Ozawa, and S. Yamamoto, Appl. Surf. Sci. **146**, 158 (1999).

[13] J. Tersoff and D. R. Hamman, Phys. Rev. B **31**, 805 (1985).

[14] K. Kobayashi, Phys. Rev. B **53**, 11 091 (1996).

[15] U. Starke, A. Barbier, N. Materer, M. A. Van Hove, and G. A. Somorjai, Surf. Sci. **286**, 1 (1993).

[16] L. Olesen, M. Brandbyge, M. R. Sørensen, K. W. Jacobsen, E. Lægsgaard, I. Stensgaard, and F. Bensenbacher, Phys. Rev. Lett. **76**, 1485 (1996).